EUROPEAN ORGANIZATION FOR NUCLEAR RESEARCH

CERN-PPE/92-104

25 June 1992

Evidence for B_s^0 Meson Production in Z^0 Decays

DELPHI Collaboration

Abstract

Seven unambiguous events out of a sample of 270 000 Z^0 decays, contain in the same jet a D_s meson and a muon at large transverse momentum relative to the jet axis. These events are direct evidence for B_s^0 meson production in hadronic Z^0 decays. The production rate of these events, relative to all hadronic Z^0 decays is $(18 \pm 8) \times 10^{-5}$, this number including the relevant branching fractions of the B_s^0 and D_s. The value of the B_s^0 meson lifetime relative to the average B meson lifetime is measured to be 0.8 ± 0.4 .

(Submitted to Physics Letters B)

P.Abreu[19], W.Adam[46], T.Adye[34], E.Agasi[28], G.D.Alekseev[13], P.Allen[45], S.Almehed[22], S.J.Alvsvaag[4], U.Amaldi[7], E.G.Anassontzis[3], A.Andreazza[26], P.Antilogus[23], W-D.Apel[14], R.J.Apsimon[34], B.Åsman[41], J-E.Augustin[17], A.Augustinus[28], P.Baillon[7], P.Bambade[17], F.Barao[19], R.Barate[11], G.Barbiellini[43], D.Y.Bardin[13], A.Baroncelli[37], O.Barring[22], J.A.Barrio[24], W.Bartl[46], M.J.Bates[31], M.Battaglia[26], M.Baubillier[21], K-H.Becks[48], C.J.Beeston[31], M.Begalli[33], P.Beilliere[6], Yu.Belokopytov[39], K.Belous[39], P.Beltran[9], D.Benedic[8], A.C.Benvenuti[5], M.Berggren[17], D.Bertrand[2], F.Bianchi[42], M.S.Bilenky[13], P.Billoir[21], J.Bjarne[22], D.Bloch[8], S.Blyth[31], V.Bocci[35], P.N.Bogolubov[13], T.Bolognese[36], M.Bonesini[26], W.Bonivento[26], P.S.L.Booth[20], P.Borgeaud[36], G.Borisov[39], H.Borner[7], C.Bosio[37], B.Bostjancic[7], S.Bosworth[31], O.Botner[44], B.Bouquet[17], C.Bourdarios[17], T.J.V.Bowcock[20], M.Bozzo[10], S.Braibant[2], P.Branchini[37], K.D.Brand[32], R.A.Brenner[7], H.Briand[21], C.Bricman[2], R.C.A.Brown[7], N.Brummer[28], J-M.Brunet[6], L.Bugge[30], T.Buran[30], H.Burmeister[7], J.A.M.A.Buytaert[2], M.Caccia[7], M.Calvi[26], A.J.Camacho Rozas[38], T.Camporesi[7], V.Canale[35], F.Cao[2], F.Carena[7], L.Carroll[20], C.Caso[10], E.Castelli[43], M.V.Castillo Gimenez[45], A.Cattai[7], F.R.Cavallo[5], L.Cerrito[35], V.Chabaud[7], A.Chan[1], M.Chapkin[39], Ph.Charpentier[7], L.Chaussard[17], J.Chauveau[21], P.Checchia[32], G.A.Chelkov[13], L.Chevalier[36], P.Chliapnikov[39], V.Chorowicz[21], J.T.M.Chrin[45], R.Cirio[42], M.P.Clara[42], P.Collins[31], J.L.Contreras[24], R.Contri[10], E.Cortina[45], G.Cosme[17], F.Couchot[17], H.B.Crawley[1], D.Crennell[34], G.Crosetti[10], M.Crozon[6], J.Cuevas Maestro[38], S.Czellar[12], S.Dagoret[17], E.Dahl-Jensen[27], B.Dalmagne[17], M.Dam[30], G.Damgaard[27], G.Darbo[10], E.Daubie[2], A.Daum[14], P.D.Dauncey[31], M.Davenport[7], P.David[21], W.Da Silva[21], C.Defoix[6], D.Delikaris[7], B.A.Della Riccia[42], S.Delorme[7], P.Delpierre[6], N.Demaria[42], A.De Angelis[43], M.De Beer[36], H.De Boeck[2], W.De Boer[14], C.De Clercq[2], M.D.M.De Fez Laso[45], N.De Groot[28], C.De La Vaissiere[21], B.De Lotto[43], A.De Min[26], H.Dijkstra[7], L.Di Ciaccio[35], F.Djama[8], J.Dolbeau[6], M.Donszelmann[7], K.Doroba[47], M.Dracos[7], J.Drees[48], M.Dris[29], Y.Dufour[6], R.Dzhelyadin[39], L-O.Eek[44], P.A.-M.Eerola[7], R.Ehret[14], T.Ekelof[44], G.Ekspong[41], A.Elliot Peisert[32], J-P.Engel[8], D.Fassouliotis[29], T.A.Fearnley[4], M.Feindt[7], A.Fenyuk[39], M.Fernandez Alonso[38], A.Ferrer[45], T.A.Filippas[29], A.Firestone[1], H.Foeth[7], E.Fokitis[29], F.Fontanelli[10], K.A.J.Forbes[20], J-L.Fousset[25], B.Franek[34], P.Frenkiel[6], D.C.Fries[14], A.G.Frodesen[4], R.Fruhwirth[46], F.Fulda-Quenzer[17], K.Furnival[20], H.Furstenau[14], J.Fuster[7], G.Galeazzi[32], D.Gamba[42], C.Garcia[45], J.Garcia[38], C.Gaspar[7], U.Gasparini[32], Ph.Gavillet[7], E.N.Gazis[29], J-P.Gerber[8], P.Giacomelli[7], R.Gokieli[47], B.Golob[40], V.M.Golovatyuk[13], J.J.Gomez Y Cadenas[7], A.Goobar[41], G.Gopal[34], M.Gorski[47], V.Gracco[10], A.Grant[7], F.Grard[2], E.Graziani[37], G.Grosdidier[17], E.Gross[7], P.Grosse-Wiesmann[7], B.Grossetete[21], S.Gumenyuk[39], J.Guy[34], U.Haedinger[14], F.Hahn[48], M.Hahn[14], S.Haider[28], Z.Hajduk[15], A.Hakansson[22], A.Hallgren[44], K.Hamacher[48], G.Hamel De Monchenault[36], W.Hao[28], F.J.Harris[31], T.Henkes[7], J.J.Hernandez[45], P.Herquet[2], H.Herr[7], T.L.Hessing[20], I.Hietanen[12], C.O.Higgins[20], E.Higon[45], H.J.Hilke[7], S.D.Hodgson[31], T.Hofmokl[47], R.Holmes[1], S-O.Holmgren[41], D.Holthuizen[28], P.F.Honore[6], J.E.Hooper[27], M.Houlden[20], J.Hrubec[46], P.O.Hulth[41], K.Hultqvist[41], P.Ioannou[3], D.Isenhower[7], P-S.Iversen[4], J.N.Jackson[20], P.Jalocha[15], G.Jarlskog[22], P.Jarry[36], B.Jean-Marie[17], E.K.Johansson[41], D.Johnson[20], M.Jonker[7], L.Jonsson[22], P.Juillot[8], G.Kalkanis[3], G.Kalmus[34], F.Kapusta[21], M.Karlsson[7], E.Karvelas[9], A.Katargin[39], S.Katsanevas[3], E.C.Katsoufis[29], R.Keranen[12], J.Kesteman[2], B.A.Khomenko[13], N.N.Khovanski[13], B.King[20], N.J.Kjaer[7], H.Klein[7], W.Klempt[7], A.Klovning[4], P.Kluit[28], A.Koch-Mehrin[48], J.H.Koehne[14], B.Koene[28], P.Kokkinias[9], M.Kopf[14], K.Korcyl[15], A.V.Korytov[13], V.Kostioukhine[39], C.Kourkoumelis[3], O.Kouznetsov[13], P.H.Kramer[48], J.Krolikowski[47], I.Kronkvist[22], J.Krstic[31], U.Kruener-Marquis[48], W.Krupinski[15], K.Kulka[44], K.Kurvinen[12], C.Lacasta[45], C.Lambropoulos[9], J.W.Lamsa[1], L.Lanceri[43], V.Lapin[39], J-P.Laugier[36], R.Lauhakangas[12], G.Leder[46], F.Ledroit[11], R.Leitner[7], Y.Lemoigne[36], J.Lemonne[2], G.Lenzen[48], V.Lepeltier[17], J.M.Levy[8], E.Lieb[48], D.Liko[46], E.Lillethun[4], J.Lindgren[12], R.Lindner[48], A.Lipniacka[47], I.Lippi[32], B.Loerstad[22], M.Lokajicek[13], J.G.Loken[31], A.Lopez-Fernandez[17], M.A.Lopez Aguera[38], M.Los[28], D.Loukas[9], J.J.Lozano[45], P.Lutz[6], L.Lyons[31], G.Maehlum[7], J.Maillard[6], A.Maio[19], A.Maltezos[9], F.Mandl[46], J.Marco[38], M.Margoni[32], J-C.Marin[7], A.Markou[9], T.Maron[48], S.Marti[45], L.Mathis[1], F.Matorras[38], C.Matteuzzi[26], G.Matthiae[35], M.Mazzucato[32], M.Mc Cubbin[20], R.Mc Kay[1], R.Mc Nulty[20], G.Meola[10], C.Meroni[26], W.T.Meyer[1], M.Michelotto[32], I.Mikulec[46], W.A.Mitaroff[46], G.V.Mitselmakher[13], U.Mjoernmark[22], T.Moa[41], R.Moeller[27], K.Moenig[7], M.R.Monge[10], P.Morettini[10], H.Mueller[14], W.J.Murray[34], B.Muryn[17], G.Myatt[31], F.Naraghi[21], F.L.Navarria[5], P.Negri[26], B.S.Nielsen[27], B.Nijjhar[20], V.Nikolaenko[39], P.E.S.Nilsen[4], P.Niss[41], V.Obraztsov[39], A.G.Olshevski[13], R.Orava[12], A.Ostankov[39], K.Osterberg[12], A.Ouraou[36], M.Paganoni[26], R.Pain[21], H.Palka[28], Th.D.Papadopoulou[29], L.Pape[7], A.Passeri[37], M.Pegoraro[32], J.Pennanen[12], L.Peralta[19], V.Perevoschikov[39], M.Pernicka[46], A.Perrotta[5], A.Petrolini[10], T.E.Pettersen[32], F.Pierre[36], M.Pimenta[19], O.Pingot[2], M.E.Pol[7], G.Polok[15], P.Poropat[43], P.Privitera[14], A.Pullia[26], D.Radojicic[31], S.Ragazzi[26], P.N.Ratoff[18], A.L.Read[30], N.G.Redaelli[26], M.Regler[46], D.Reid[20], P.B.Renton[31], L.K.Resvanis[3], F.Richard[17], M.Richardson[20], J.Ridky[13], G.Rinaudo[42], I.Roditi[16], A.Romero[42], I.Roncagliolo[10], P.Ronchese[32], V.Ronjin[39], C.Ronnqvist[12], E.I.Rosenberg[1], S.Rossi[7], U.Rossi[5], E.Rosso[7], P.Roudeau[17], T.Rovelli[5], W.Ruckstuhl[28], V.Ruhlmann[36], A.Ruiz[38], K.Rybicki[15], H.Saarikko[12], Y.Sacquin[36], G.Sajot[11], J.Salt[45], J.Sanchez[24], M.Sannino[10], S.Schael[14], H.Schneider[14], M.A.E.Schyns[48], G.Sciolla[42], F.Scuri[43], A.M.Segar[31], R.Sekulin[34], M.Sessa[43], G.Sette[10],

R.Seufert[14], R.C.Shellard[33], I.Siccama[28], P.Siegrist[36], S.Simonetti[10], F.Simonetto[32], A.N.Sisakian[13], T.B.Skaali[30], G.Skjevling[30], G.Smadja[36,23], N.Smirnov[39], G.R.Smith[34], R.Sosnowski[47], T.S.Spassoff[11], E.Spiriti[37], S.Squarcia[10], H.Staeck[48], C.Stanescu[37], S.Stapnes[30], G.Stavropoulos[9], F.Stichelbaut[2], A.Stocchi[17], J.Strauss[46], J.Straver[7], R.Strub[8], M.Szczekowski[47], M.Szeptycka[47], P.Szymanski[47], T.Tabarelli[26], S.Tavernier[2], O.Tchikilev[39], G.E.Theodosiou[9], A.Tilquin[25], J.Timmermans[28], V.G.Timofeev[13], L.G.Tkatchev[13], T.Todorov[8], D.Z.Toet[28], O.Toker[12], A.Tomaradze[39], B.Tome[19], E.Torassa[42], L.Tortora[37], M.T.Trainor[31], D.Treille[7], U.Trevisan[10], W.Trischuk[7], G.Tristram[6], C.Troncon[26], A.Tsirou[7], E.N.Tsyganov[13], M.Turala[15], M-L.Turluer[36], T.Tuuva[12], I.A.Tyapkin[21], M.Tyndel[34], S.Tzamarias[7], S.Ueberschaer[48], O.Ullaland[7], V.Uvarov[39], G.Valenti[5], E.Vallazza[42], J.A.Valls Ferrer[45], C.Vander Velde[2], G.W.Van Apeldoorn[28], P.Van Dam[28], W.K.Van Doninck[2], P.Vas[7], G.Vegni[26], L.Ventura[32], W.Venus[34], F.Verbeure[2], L.S.Vertogradov[13], D.Vilanova[36], N.Vishnevsky[39], L.Vitale[12], E.Vlasov[39], A.S.Vodopyanov[13], M.Vollmer[48], G.Voulgaris[3], M.Voutilainen[12], V.Vrba[37], H.Wahlen[48], C.Walck[41], F.Waldner[43], M.Wayne[1], A.Wehr[48], M.Weierstall[48], P.Weilhammer[7], J.Werner[48], A.M.Wetherell[7], J.H.Wickens[2], J.Wikne[30], G.R.Wilkinson[31], W.S.C.Williams[31], M.Winter[8], D.Wormald[30], G.Wormser[17], K.Woschnagg[44], N.Yamdagni[41], P.Yepes[7], A.Zaitsev[39], A.Zalewska[15], P.Zalewski[17], D.Zavrtanik[7], E.Zevgolatakos[9], G.Zhang[48], N.I.Zimin[13], M.Zito[36], R.Zuberi[31], R.Zukanovich Funchal[6], G.Zumerle[32], J.Zuniga[45]

[1] Ames Laboratory and Department of Physics, Iowa State University, Ames IA 50011, USA
[2] Physics Department, Univ. Instelling Antwerpen, Universiteitsplein 1, B-2610 Wilrijk, Belgium
and IIHE, ULB-VUB, Pleinlaan 2, B-1050 Brussels, Belgium
and Faculté des Sciences, Univ. de l'Etat Mons, Av. Maistriau 19, B-7000 Mons, Belgium
[3] Physics Laboratory, University of Athens, Solonos Str. 104, GR-10680 Athens, Greece
[4] Department of Physics, University of Bergen, Allégaten 55, N-5007 Bergen, Norway
[5] Dipartimento di Fisica, Università di Bologna and INFN, Via Irnerio 46, I-40126 Bologna, Italy
[6] Collège de France, Lab. de Physique Corpusculaire, 11 pl. M. Berthelot, F-75231 Paris Cedex 05, France
[7] CERN, CH-1211 Geneva 23, Switzerland
[8] Centre de Recherche Nucléaire, IN2P3 - CNRS/ULP - BP20, F-67037 Strasbourg Cedex, France
[9] Institute of Nuclear Physics, N.C.S.R. Demokritos, P.O. Box 60228, GR-15310 Athens, Greece
[10] Dipartimento di Fisica, Università di Genova and INFN, Via Dodecaneso 33, I-16146 Genova, Italy
[11] Institut des Sciences Nucléaires, Université de Grenoble 1, F-38026 Grenoble, France
[12] Research Institute for High Energy Physics, SEFT, Siltavuorenpenger 20 C, SF-00170 Helsinki, Finland
[13] Joint Institute for Nuclear Research, Dubna, Head Post Office, P.O. Box 79, 101 000 Moscow, USSR.
[14] Institut für Experimentelle Kernphysik, Universität Karlsruhe, Postfach 6980, D-7500 Karlsruhe 1, FRG
[15] High Energy Physics Laboratory, Institute of Nuclear Physics, Ul. Kawiory 26 a, PL-30055 Krakow 30, Poland
[16] Centro Brasileiro de Pesquisas, rua Xavier Sigaud 150, RJ-22290 Rio de Janeiro, Brazil
[17] Université de Paris-Sud, Lab. de l'Accélérateur Linéaire, Bat 200, F-91405 Orsay, France
[18] School of Physics and Materials, University of Lancaster - Lancaster LA1 4YB, UK
[19] LIP, IST, FOUL - Av. Elias Garcia, 14 - 1°, P-1000 Lisboa Codex, Portugal
[20] Department of Physics, University of Liverpool, P.O. Box 147, GB - Liverpool L69 3BX, UK
[21] LPNHE, Universités Paris VI et VII, Tour 33 (RdC), 4 place Jussieu, F-75230 Paris Cedex 05, France
[22] Department of Physics, University of Lund, Sölvegatan 14, S-22363 Lund, Sweden
[23] Université Claude Bernard de Lyon, 43 Bd du 11 Novembre 1918, F-69622 Villeurbanne Cedex, France
[24] Universidad Complutense, Avda. Complutense s/n, E-28040 Madrid, Spain
[25] Univ. d'Aix - Marseille II - Case 907 - 70, route Léon Lachamp, F-13288 Marseille Cedex 09, France
[26] Dipartimento di Fisica, Università di Milano and INFN, Via Celoria 16, I-20133 Milan, Italy
[27] Niels Bohr Institute, Blegdamsvej 17, DK-2100 Copenhagen 0, Denmark
[28] NIKHEF-H, Postbus 41882, NL-1009 DB Amsterdam, The Netherlands
[29] National Technical University, Physics Department, Zografou Campus, GR-15773 Athens, Greece
[30] Physics Department, University of Oslo, Blindern, N-1000 Oslo 3, Norway
[31] Nuclear Physics Laboratory, University of Oxford, Keble Road, GB - Oxford OX1 3RH, UK
[32] Dipartimento di Fisica, Università di Padova and INFN, Via Marzolo 8, I-35131 Padua, Italy
[33] Depto. de Fisica, Pontificia Univ. Católica, C.P. 38071 RJ-22453 Rio de Janeiro, Brazil
[34] Rutherford Appleton Laboratory, Chilton, GB - Didcot OX11 OQX, UK
[35] Dipartimento di Fisica, Università di Roma II and INFN, Tor Vergata, I-00173 Rome, Italy
[36] CEN-Saclay, DPhPE, F-91191 Gif-sur-Yvette Cedex, France
[37] Istituto Superiore di Sanità, Ist. Naz. di Fisica Nucl. (INFN), Viale Regina Elena 299, I-00161 Rome, Italy
[38] Facultad de Ciencias, Universidad de Santander, av. de los Castros, E - 39005 Santander, Spain
[39] Inst. for High Energy Physics, Serpukow P.O. Box 35, Protvino, (Moscow Region), CEI
[40] Institut "Jozef Stefan", Ljubljana, Slovenija
[41] Institute of Physics, University of Stockholm, Vanadisvägen 9, S-113 46 Stockholm, Sweden
[42] Dipartimento di Fisica Sperimentale, Università di Torino and INFN, Via P. Giuria 1, I-10125 Turin, Italy
[43] Dipartimento di Fisica, Università di Trieste and INFN, Via A. Valerio 2, I-34127 Trieste, Italy
and Istituto di Fisica, Università di Udine, I-33100 Udine, Italy
[44] Department of Radiation Sciences, University of Uppsala, P.O. Box 535, S-751 21 Uppsala, Sweden
[45] IFIC, Valencia-CSIC, and D.F.A.M.N., U. de Valencia, Avda. Dr. Moliner 50, E-46100 Burjassot (Valencia), Spain
[46] Institut für Hochenergiephysik, Österr. Akad. d. Wissensch., Nikolsdorfergasse 18, A-1050 Vienna, Austria
[47] Inst. Nuclear Studies and, University of Warsaw, Ul. Hoza 69, PL-00681 Warsaw, Poland
[48] Fachbereich Physik, University of Wuppertal, Postfach 100 127, D-5600 Wuppertal 1, FRG

1 Introduction

The presence of the B_s^0 meson†, carrying both beauty and strangeness, at e^+e^- or $p\bar{p}$ colliders has been up to now inferred from the measurement of the rate of same sign dileptons[1]. This rate is larger than the corresponding value[2] obtained at the $\Upsilon(4S)$ and this difference can be explained by the production, at a rate around 12%, of strange B_s^0 mesons which undergo a complete $B_s^0 - \overline{B_s^0}$ mixing. Evidence for B_s^0 production was also obtained by the CUSB collaboration from data registered at the $\Upsilon(5S)$[3]. No measurement exists yet on the decay properties of the B_s^0 meson.

This paper shows that samples containing mainly B_s^0 decay products can be isolated at LEP, opening new possibilities for the study of the properties of this particle. A sample of 270000 hadronic Z^0 decays registered by DELPHI in 1991 has been used for this analysis.

2 Isolation of B_s^0 mesons

The observed B_s^0 mesons were produced during the hadronization of b quark jets emitted in the decay of a Z^0 boson. From the measured production rate of strange particles in hadronic jets, the probability to get an $s\bar{s}$ pair at each step of the hadronization chain is estimated of the order of 12%[4]. In the case of semi-leptonic decays, as explained below, events containing in the same jet a D_s meson and a lepton at large transverse momentum relative to the jet axis are essentially pure manifestations of B_s^0 meson decays. The visibility of the signal from B_s^0 mesons is mainly determined by two parameters: the probability that a D_s meson is produced in a semi-leptonic decay of a B_s^0 particle and the background probability that non-strange B particles emit a lepton and a D_s meson in a direct or a cascade semi-leptonic decay.

Four processes, all from B decays, contribute to the production of the $\ell^\pm D_s^\mp X$ final state with the lepton and the strange D_s meson observed in the same jet. Two come from direct B meson semi-leptonic decays and the others from semi-leptonic cascade decays of B hadrons as shown in figure 1.

The process in Fig. 1-a corresponds to the signal. The B_s^0 meson decays into $\ell^\pm D_s^\mp \nu_l$ or into $\ell^\pm D_s^{*\mp} \nu_l$ followed by the decay $D_s^* \to D_s\gamma$. The contributions from non-resonant hadronic final states and from D_s^{**} mesons are not expected to give large contributions to the signal because these channels give rise mainly to D^0KX or to D^+KX events. The fraction of D_s^{**}-like states that decays into a D_s meson is expected to be of the order of 20%: 10% are produced by violation of the Zweig rule in the sector of strange quarks and the remaining 10% come from the usual strange particle production in hadronic systems. In the case of non-strange B mesons, current theoretical expectations [5] [6] predict values in the range 10 to 25 % for the fraction of D^{**} or non-resonant $D(n\pi)$ final states in the semi-leptonic decays of B_d^0 or B^+ mesons. These predictions are somewhat lower than present measurements from the ARGUS and CLEO collaborations[7] which found a value of $40 \pm 10\%$.

In the following it is assumed that 25% of the B_s^0 semi-leptonic decays go through D_s^{**} or non-resonant $D(n\pi)$ so that:

$$\frac{BR(B_s \to D_s \ell\nu X)}{BR(B_s \to \ell\nu X)} = 0.80 \ .$$

Process 1-b is the semi-leptonic decay of a non-strange B meson to a hadronic system including a D_s and a K mesons. Here the fraction of the events with a strange D_s

† Throughout this paper the symbol for a particle is taken to include the corresponding antiparticle, unless explicitly stated otherwise.

meson will be smaller than the usual probability of extracting strange quarks from the sea because of the further limitation from phase-space. The distribution of the mass of the hadronic system produced in a semi-leptonic decay of a B hadron falls steeply at high values and the threshold for $D_s - K$ production is situated in the far tail of the distribution, above the nominal mass values of possible D** states. A detailed theoretical analysis, based on the quark model, and using the evaluation of the transitions of the B meson to individual D, D* and higher D** resonances can be found in reference [6]. The expected production of D_sKX final states is rather stable to variations of the parameters of the model. In particular there is no direct correlation between the fractions expected for D_sKX and D** final states and the following limit is obtained:

$$\frac{BR(B_d,B^+ \to D_s \ell\nu X)}{BR(B_d \to \ell\nu X)} \leq 0.025 \ .$$

This gives an upper limit of 20% for the contribution of the diagram 1-b relative to the process 1-a (Table 1) and, in the following analysis, this process has been neglected.

Processes 1-c and 1-d correspond to semi-leptonic cascade decays of B mesons into final states with two charmed particles. A D_s meson is formed through the coupling of the virtual W to $c\bar{s}$ quark pairs. This coupling is Cabibbo favoured but it is penalized, relative to the coupling to $u\bar{d}$ quark pairs, by the phase space limitations coming from the heavier masses of the c and $\bar{s}$ quarks as compared to u and $\bar{d}$ masses. ARGUS and CLEO have measured:[7]

$$BR(B \to D_sX) = (10 \pm 2 \pm 4)\%$$

(in this expression B means 50% neutral and 50% charged B's and a branching fraction of $(3.1^{+1.2}_{-1.0})$ % is assumed for the D_s decay into $\phi\pi$ [8]). B_s^0 meson decays contribute simultaneously to processes 1-c and 1-d because the lepton can be produced from one of the two D_s mesons that are present.

Contribution from $Z^0 \to c\bar{c}$ events is only expected through the presence of misidentified hadrons in the sample of muon candidates. The contribution from these classes of events can be evaluated in the data because similar numbers of $l^{\pm}D_s^{\mp}$ and of $l^{\mp}D_s^{\mp}$ candidates are expected from this source. This applies also to the candidates coming from the combinatorial background present under the D_s mass peak.

Table 1: *Contribution of each process to the l D_s correlation. Prob(B) is the probability to find the proper B meson in a b jet. Prob(l) is the corresponding semi-leptonic branching fraction. Prob(D_s) is the probability to get a D_s meson in the semi-leptonic decay.*

diagram	Prob(B)	Prob(l)	Prob(D_s)	Prob. per had. event
1-a	0.12	0.1	0.80	$4.22\ 10^{-3}$
1-b	0.75	0.1	≤ 0.025	$\leq 0.82\ 10^{-3}$
1-c	1.0	$\simeq 0.1$	0.1	$4.4\ 10^{-3}$
1-d	0.12	$\simeq 0.1$	0.1	$0.52\ 10^{-3}$

Table 1 gives rough estimates of the relative contributions from the different processes, prior to any reduction from detection efficiencies. Before any cut to identify the lepton and the D_s meson, similar numbers of events are expected from processes 1-a and 1-c.

However, the leptons emitted from the cascade decay process 1-c are softer and have a lower transverse momentum[‡] than those from process 1-a. Differences in acceptance,

[‡]The transverse momentum of the lepton is measured relative to the axis of the hadronic system present in the jet, in addition to the lepton. Jets have been reconstructed using the LUND LUCLUS algorithm[9] with default parameters.

and proper cuts on the kinematical variables will thus modify the contributions from the different classes in the sample of selected events. For example, at a transverse momentum of the lepton P_t above 1.2 GeV/c, more than 90 % of the events are expected to originate from B_s^0 semi-leptonic decays, if process 1-b is neglected. This can be seen on figure 2 which shows the Monte Carlo simulated lepton P_t distribution in Z^0 decays, dominated by the processes of figure 1, and which includes acceptance and detection efficiencies.

3 Detector

The components of the DELPHI detector which play an important role in the present analysis are described here. A complete description of the DELPHI apparatus is given in reference [10].

The muon identification relied mainly on the muon chambers, a set of drift chambers providing three dimensional information. In the barrel part of the detector, covering polar angles between 52° and 128° , there are 3 sets of chambers. One set of chambers is located just inside the hadron calorimeter and two sets are just beyond it, with 2 layers of chambers in each set. The third set, which completes the azimuthal coverage, has a small overlap with the others. The forward muon chambers cover polar angles between 9° to 43° and 137° to 171°. Both arms have two planes of chambers; one inside the yoke, behind more than 85 cm of iron, the second 30 cm further out, behind another 20 cm of iron.

The central tracking system, composed of the Inner Detector (ID), the Time Projection Chamber (TPC) and the Outer Detector (OD), measured the tracks at polar angle larger than 30° with a resolution of $\frac{\sigma(p)}{p} \simeq 0.002 \times p$. The TPC is the main tracking device. It is a cylinder of 30 cm inner radius, 122 cm outer radius and has a length of 2.7 m. For polar angles between 39° and 141° up to 16 space points can be used. The energy loss (dE/dx) for each charged particle is measured by the 192 TPC sense wires as the 80% truncated mean of the maximum amplitudes of the wires signals. By using $Z^0 \rightarrow \mu^+\mu^-$ events, the dE/dx resolution has been measured to be 5.5%. For tracks in hadronic jets the resolution is 7.5%, and 25% of the tracks have no information because they are too close to another track.

The MicroVertex detector (VD) consists of three concentric shells of Si-strip detectors at average radii of 6.3, 9 and 11 cm covering the central region of the DELPHI apparatus at polar angles between 27° and 153°. The shells surround the beam pipe, a beryllium cylinder 1.45 mm thick with a 5.3 cm inner radius. Each shell consists of 24 modules with about 10% overlap in azimuth between the modules. Each module carries 4 detectors with strips parallel to the beam direction. The silicon detectors are 300 μm thick and have a diode pitch of 25 μm. A new feature is that the read-out strips (50 μm pitch) are AC coupled giving a 5 μm intrinsic precision on the coordinates of the charged tracks, transverse to the beam direction.

After a careful procedure of relative alignment of each single detector, an overall precision of 8 μm has been achieved. By using the combined information from OD+TPC+ID+VD a resolution of 3.5% on $\frac{\sigma(p)}{p}$ was obtained for 45 GeV/c muons.

4 Analysis

In the study of D_s-lepton correlations in the same jet, only identified muons were used. Muons were selected if their momentum was larger than 3 GeV/c and if they

were identified using the information from the muon chambers. A detailed description of the algorithm used for this selection can be found in reference [11]. The overall muon identification efficiency was measured with the $Z^0 \rightarrow \mu^+\mu^-$ final state. In the solid angle of interest in this analysis, which includes an incomplete coverage by the muon chambers near 45° and 135°, a mean efficiency of $69 \pm 2\%$ was obtained. It has been verified, using the DELPHI Monte Carlo simulation program, that the ambiguities arising from neighbouring particles do not reduce the identification efficiency inside a jet.

All charged particles were separated into two hemispheres by the plane normal to the thrust axis of the event and containing the beam interaction point. The event primary vertex was determined using all charged tracks with momentum larger than 500 MeV/c, except the lepton candidate. The vertex position had to be compatible with the beam spot position which was measured for each LEP fill. If it was not, an iterative procedure was used to eliminate from the tracks used in the vertex evaluation those which gave the largest contribution to the χ^2. From Monte Carlo simulated $b\bar{b}$ events it was verified that the accuracy on the main vertex reconstruction was 80 μm in the horizontal direction, in which the beam spot had its largest extension, and 40 μm in the vertical direction.

D_s mesons were searched for using the $\phi\pi$ and K^{*0} K decay modes, with only charged particles in the final state. The three tracks were selected in the same hemisphere as the muon and their momentum was required to be larger than 2 GeV/c. These tracks had also to be associated to hits in the silicon vertex detector and they had to intersect at a common secondary vertex. To reduce the combinatorial background, a positive decay length was required between the secondary and main vertices. The accuracy on the secondary vertex reconstruction measured on the simulated data was 300μm along the flight direction of the D_s meson and 30 μm in the perpendicular direction.

Mass combinations were obtained by requiring that a K^+K^- combination was in the ϕ region, between 1.012 and 1.028 GeV/c^2, or a K π system in the K^{*0} region, between 0.83 and 0.95 GeV/c^2. For the K^{*0}, the kaon mass was attributed to the particle which had the same charge as the lepton. The third particle was then selected if it had a charge opposite to that of the lepton. These assignments were not always correct for the combinatorial background, and therefore particle identification was used to reduce it.

Loose cuts were applied on particle identification. No selection was applied on the two kaons from the ϕ decay because the two tracks are too close and most of the time cannot be identified separately. In the K^{*0} decay it was required that the dE/dx of the candidate kaon be smaller than the value associated to the candidate pion. From Monte Carlo simulation it has been verified that, in the case of genuine K^{*0} decays, this condition was fulfilled in 70% of the cases. The remaining kaon, in the $K^{*0}K$ decay, had to have a dE/dx compatible with the kaon hypothesis. The measured dE/dx value must not exceed by more than 12% (1.5 standard deviations) the expected value for a kaon having the same momentum. If no dE/dx information was available the particle was kept.

The D_s is a pseudo-scalar meson and, in this analysis, it decays into a vector and a pseudoscalar mesons. Because of helicity conservation, in the rest frame of the vector meson, the angle ψ between its decay products and the direction of the bachelor pseudoscalar has a $\cos^2\psi$ distribution. In the following, events were selected with $|\cos\psi| \geq 0.5$. This cut keeps 88% of the signal, if possible acceptance distortions are neglected.

Taking events in the ϕ and in the K^{*0} mass regions, a signal centered on the D_s mass was visible both in the $\phi\pi$ and $K^{*0}K$ mass distributions. Figure 3 shows these signals when the D_s was associated to a muon with a transverse momentum larger than 0.6 GeV/c. The $\phi\pi$ and $K^{*0}K$ mass distributions were summed in the analysis which follows. It was

verified that the two distributions contained no common candidates. These distributions are shown for P_t cuts of 0.8 GeV/c in figure 3-c, and 1.2 GeV/c in figure 3-d.

4.1 Study of B_s^0 meson production

The statistical evidence for the D_s signal depends upon the knowledge of the values for the mass and width of the D_s particle as reconstructed by the DELPHI detector. These values were obtained by searching for inclusive D_s meson production in hadronic jets. In the $\phi\pi$ decay channel a signal of 74 ± 15 events was observed with the following parameters:

$$M_{D_s} = 1963 \pm 2 \text{ MeV/c}^2 \ , \quad \sigma_{M_{D_s}} = 6.9 \pm 1.3 \text{ MeV/c}^2$$

The mean value of the D_s mass was lower than the nominal value by 6 MeV/c^2. A similar displacement was also observed for the D^0 mass peak and it was attributed to remaining defects in the detector alignment. The D_s reconstructed width was narrower than the Monte Carlo simulation estimate which was 11 MeV/c^2. In order to evaluate the statistical significance of the observed accumulation of events in a given mass distribution, the probability to get at least the measured number of events in a region centered on the expected D_s mass and having a width equal to 30 MeV/c^2 was computed. This mass interval contains about 85% of the signal if the mass resolution is equal to 11 MeV/c^2. A binomial probability distribution was used and for the two selected samples of events shown in figs. 3-c and 3-d, the respective probabilities are 1.3×10^{-3} and 2.1×10^{-4}.

An unbinned maximum likelihood fit of a gaussian distribution for the signal, with a fixed width to 11 MeV/c^2, and a linear background gave the following mass and number of events on the data selected with the P_t cut of 1.2 GeV/c:

$$M_{D_s} = 1965.6 \pm 5.1 \text{ MeV/c}^2$$

$$N_{D_s} = 7.5 \ ^{+3.3}_{-2.6} \qquad N_{D_s} \geq 3.7 \text{ at 95\% confidence level}$$

The value obtained for the mass is compatible with the corresponding measured value using the inclusive D_s signal.

It was also verified that the accumulation of events around the D_s mass was not due to the reflection of other charm hadronic decays. The main candidate for such a spurious peak is the D^+ which decays into $K^-\pi^+\pi^+$ and in which one of the charged pions is taken as a kaon. Events were selected with a muon with a transverse momentum larger than 1.2 GeV/c and with a $K\pi$ invariant mass in the K^{*0} region (figure 4-a). Possible mass reflections coming from the $\phi\pi$ decay channel have been neglected because of the narrowness of the ϕ signal. Cuts on the ψ angle, on particle identification, and on the flight distance were then applied and 3 events remained (figure 4-b) which were compatible with a narrow mass peak centered around the D^+ mass. In the $K^{*0}K$ mass distribution, a genuine D^+ decaying into $K\pi\pi$ would appear as a broad accumulation of total width 200 MeV/c^2 extending above the D_s nominal mass. In fig. 4-c these 3 events are shown in the $KK\pi$ hypothesis using a binning of 10 MeV/c. Because of the narrowness of the genuine D_s signal two of them are not compatible with the D_s hypothesis and one is ambiguous. In the selected range of transverse momentum there are thus 7 events coming unambiguously from D_s decays.

Using the result from the fit of the mass distribution given previously and the expected contributions from the different mechanisms shown in fig. 2, the number of

events coming exclusively from the direct semi-leptonic decay $B_s \rightarrow \mu D_s X \nu$ is then: $N_{B_s \rightarrow D_s \mu \nu X}(P_t^{\mu} > 1.2 GeV/c) = 5.4 \, ^{+2.7}_{-2.1}$ and is larger than 2.2 at the 95% confidence level.

The same analysis was repeated to check the charge relation between the muon and the D_s. As explained in section 2, same-sign muon-D_s correlations come from misidentified muons or from the combinatorial background under the D_s peak. In figure 5-a, the $KK\pi$ mass distribution of these same sign events containing a ϕ or K^{*0} mass is shown: no accumulation exists around the D_s mass.

Other checks were also made. A cut on the $\cos\psi$ distribution, namely $|\cos\psi| \geq 0.5$, has been used. In fig.5-b the $KK\pi$ mass distribution is given for the events that were rejected by this cut. As expected, no clear signal is visible around the D_s mass. Taking events in the wings of the ϕ and of the K^{*0} mass regions, the corresponding $KK\pi$ mass distribution is given in fig. 5-c. No accumulation exists around the D_s nominal mass. Using the same mass selection but taking a muon of the same sign as the $KK\pi$ candidate, a similar distribution was obtained with slightly fewer entries (fig. 5-d).

4.2 B_s^0 production rate

To measure the B_s^0 meson production rate, the number of D_s – muon candidates was compared to the corresponding number of D^0 – muon events observed in similar conditions. This approach had the advantage that uncertainties on several parameters, such as the muon detection efficiency or the b quark fragmentation distribution, did not contribute. Also, the Monte Carlo simulation was in that case only used to correct for the differences in acceptances between the two samples of events. The D^0 was reconstructed in the $K^-\pi^+$ decay channel and events were selected if the transverse momentum of the muon was larger than 1.0 GeV/c and if the decay length was positive and larger than one standard deviation. These cuts were chosen to get a clean D^0 meson signal [12]. It contained 67 ± 10 events. In this evaluation, the following parameters (see Table 1) were used:

- probability to produce a B_s^0 meson in a b-jet equal to 12 %.
- probability to produce a B_d^0 or a B^+ meson in a b-jet equal to 75 %.
- same value for the semi-leptonic branching fraction for all B mesons.
- probability to produce a D_s meson in a B_s^0 semi-leptonic decay equal to 80 %.
- and from reference [7]: probability to produce a D^0 meson in a B_d^0 or in a B^+ semi-leptonic decay equal to 70 %.

Dedicated samples of events were generated to study the acceptance for the D_s meson decaying into $\phi\pi$ and $K^{*0}K$ respectively. Without including the muon detection efficiency which was similar for the D^0 and D_s final states, 5.5 ± 0.8% of the events were reconstructed in the $K^{*0}K$ channel, with a muon at P_t larger than 1.2 GeV/c. For the $\phi\pi$ channel, 9.9 ± 1.1% of the events were accepted. (In these simulations the K^{*0} and the ϕ mesons were generated with 100 % branching fractions into charged particles, and this was corrected for later.) For the D^0 decaying through the $K^-\pi^+$ channel, 19.9 ± 2.4% of the events were kept. The expected number of candidates from $B_s \rightarrow D_s \mu \nu X$ decays was then:

$$N_{B_s \rightarrow D_s \mu \nu X}(P_t \geq 1.2 \text{ GeV/c}) = (5.3 \pm 1.0) \times \frac{BR(D_s \rightarrow \phi\pi)}{BR(D^0 \rightarrow K^-\pi^+)}.$$

(In this expression only the statistical accuracy is quoted and the same branching fractions were assumed for the D_s meson decaying into $\phi\pi$ or $K^{*0}K$ final states.)
This evaluation is compatible with the 5.4 events events that were measured and implies that the B_s^0 production and decays are in agreement with the hypotheses listed above. If no-B_s^0 meson were produced in hadronic Z^0 decays, less than 1 event would be expected

from the semi-leptonic cascade decays of non-strange B mesons and also, less than 1 event could have been produced through the mechanism 1-b. These numbers are to be compared to the 7 candidates that were isolated.

An absolute value for the rate of production of these events has been obtained by applying acceptance and efficiency corrections and taking into account the efficiency of muon identification. It corresponds to the probability that a Z^0 boson decays into a b quark pair, that at least one of the b quarks becomes hadronized into a B_s^0 meson, that the B_s^0 undergoes a direct semi-leptonic decay giving at least one muon and a D_s meson in the final state, and that the D_s meson decays into $\phi\pi$.

$$P(Z^0 \rightarrow b \text{ or } \bar{b} \rightarrow B_s \rightarrow D_s\mu\nu X\ ,\ D_s \rightarrow \phi\pi) \ = \ (18 \pm 8) \times 10^{-5}$$

The quoted accuracy is purely of statistical origin. The systematic errors from the modelling of the b quark fragmentation and from the uncertainty on B hadron semi-leptonic decays are much smaller and have been neglected.

4.3 Expected signal from the $D^+ \rightarrow \phi\pi$ or $\rightarrow K^{*0}K$

In fixed target experiments and at e^+e^- colliders operating at lower energies the signal from the D_s is generally accompanied by a signal from the D^+ coming from the Cabibbo suppressed $KK\pi$ decay channel. The relative importance of the D_s and D^+ signals is 3:1 at the $\Upsilon(4S)$, where D mesons are produced in the inclusive decays of B^0 and B^+ mesons.

In the process we are studying, at large P_t, D_s mesons are expected to be produced from B_s^0 semi-leptonic decays whereas D^+ come from semi-leptonic decays of non-strange B mesons. The D^+ fraction in semi-leptonic B meson decays has been measured by the ARGUS and CLEO Collaborations [7]:

$$\frac{BR(B \rightarrow D^+ \ell\nu X)}{BR(B \rightarrow \ell\nu X)} = 0.26 \ \pm \ 0.07 \ \pm \ 0.04$$

The expected signal from the D^+ in the present data depends strongly on the evaluation of the ratio of the branching fractions of the D_s and of the D^+ into $\phi\pi$ and $K^{*0}K$ final states. If we take $BR(D_s \rightarrow \phi\pi) = (3.1^{+1.2}_{-1.0})\%$ as used by CLEO[8], and $BR(D^+ \rightarrow \phi\pi) = (0.57 \pm .11)\%$ as given by the Particle Data Group[13], the expected number of events in the D^+ region will be 0.42 to 0.24 times the number of events observed at the D_s mass. For P_t larger than 1.2 GeV/c this corresponds to 1.7 to 3 events when at most one event was observed. With the present statistics, this is compatible if not very significant.

Considering now the region at lower P_t, the contribution from the D^+ is only expected from the diagrams in which a B hadron decays into two D mesons, one of them being a D_s, and where a muon is produced in the semi-leptonic decay of the D_s meson. Essentially no signal from the D^+ is expected in this P_t region.

It is thus not surprising to see only a signal from the D_s meson.

4.4 Transverse momentum behaviour of the D_s signal

When the cut applied on the transverse momentum of the muon was removed, a signal of 11.5 $\pm$ 5.1 D_s events was observed, after having subtracted the possible contribution coming from the reflection of the D^+. As shown in Section 4.1, at P_t larger than 1.2 GeV/c, 7 events remain. From the Monte Carlo simulation, using the transverse momentum distribution expected for the muon (figure 2), 6.2 events are expected in the same P_t range if the full distribution is normalized to the above 11.5 events.

5 Evaluation of the lifetime of the B_s^0 meson

From the observation of unambiguous B_s^0 meson decays, it is already clear that the B_s^0 lifetime cannot be too low. A very short lifetime would imply a correspondingly small semi-leptonic branching fraction and thus no muon candidate.

The events obtained, were used to evaluate the B_s^0 lifetime. The decay length distribution of the D_s decay vertices relative to the main vertex of the event was studied and compared to the corresponding distribution obtained for the D^0 decay vertices selected in D^0-muon candidates. The topologies of these two classes of events are very similar, as are the lifetimes of the D^0 and D_s mesons. Using the mean values of the two distributions, the value of the B_s^0 meson lifetime relative to that of non-strange B mesons was measured to be:

$$\frac{\tau_{B_s^0}}{\tau_B} = 0.8 \pm 0.4.$$

At this statistical level, the measurement of this ratio will not be significantly biassed by the D lifetimes which are short compared to the B lifetime[14].

Conclusions

Seven unambiguous events containing, in the same jet, a D_s meson and a muon, with the muon at large transverse momentum relative to the jet axis, and with the D_s reconstructed through the $\phi\pi$ and $K^{*0}K$ decay channels, have been isolated in DELPHI. Less than one event was expected if no B_s^0 production was present during the hadronization of the b quark. At lower values of the muon transverse momentum the D_s signal agrees with the expectations from a Monte Carlo simulation in which D_s mesons are produced from B mesons decays.

A similar result, using the $\phi\pi$ decay mode of the D_s has been reported in the LaThuile and Moriond spring 1992 meetings by the ALEPH Collaboration, as was this result from DELPHI[15].

In a hadronic Z^0 decay final state, the probability of a B_s^0 meson to be produced and decay semi-leptonically into the $D_s\mu\nu X$ final state, with the D_s meson decaying into $\phi\pi$ has been measured to be $(18 \pm 8) \times 10^{-5}$.

From the decay length distribution of these events, the lifetime of the B_s^0 meson is found to be 0.8 ± 0.4 times the average B particle lifetime.

Acknowledgements

We are greatly indebted to our technical collaborators and to the funding agencies for their support in building and operating the DELPHI detector, and to the members of the CERN-SL Division for the excellent performance of the LEP collider. We thank A.Dobrovolskaia, A.LeYaouanc, L.Oliver, O.Pene and J.C.Raynal for useful conversations.

References

[1] C.Albajar et al., (UA1 Collaboration) Phys. Lett. B186 (1987) 247, Phys. Lett. B262 (1991) 171,
F.Abe et al., (CDF Collaboration), Phys. Rev. Lett. 67 (1991) 3351,
D.Decamp et al., (ALEPH Collaboration) Phys. Lett. B258 (1991) 236,
P.Abreu et al., (DELPHI Collaboration) to be published,
B.Adeva et al., (L3 Collaboration) Phys. Lett. B252 (1990) 703,
P.D.Acton et al., (OPAL Collaboration), Phys. Lett. B276 (1992) 379,

[2] H.Albrecht et al., (ARGUS Collaboration), Phys. Lett. B192 (1987) 247, DESY 92-050 (1992),
M.Artuso et al., (CLEO Collaboration), Phys. Rev. Lett. 62 (1989) 2233.

[3] J. Lee-Franzini et al., Phys. Rev. Lett. 65 (1990) 2947.

[4] R.P.Feynman, R.D.Field, Nucl. Phys. B136 (1978) 1,
T.Sjöstrand et al., in "Z Physics at LEP1", CERN 89-08, vol.3 (1989) 165,
P.Abreu et al., (DELPHI Collaboration) Phys. Lett. B275 (1992) 231,
G.Alexander et al., (OPAL Collaboration), Phys. Lett. B264 (1991) 467.

[5] N.Isgur, D.Scora, B.Grinstein and M.B.Wise, Phys. Rev. D39 (1989) 799.

[6] E.Golowich, A.Le Yaouanc, L.Oliver, O.Pene, J.C.Raynal, Zeit. Phys. C48 (1990) 89.

[7] K.Berkelman and S.L.Stone, Preprint CLNS 91-1044, to be published in Ann. Rev. of Nuclear and Particle Science.

[8] D.G.Cassel, in "Physics in Collision 10", A.Goshaw and L.Montanet editors, Editions Frontieres, (1990) 276.

[9] T.Sjöstrand, Comp. Phys. Comm. 27 (1982) 243, ibid. 28 (1983) 229.

[10] P.Aarnio et al., (DELPHI Collaboration) Nucl. Instr. Meth. A303 (1991) 233.

[11] P.Abreu et al., (DELPHI Collaboration) "Measurement of the Partial Width of the Z^0 into $b\bar{b}$ Final States Using their Semi-Leptonic Decays", CERN-PPE/92-79 (1992).

[12] P.Abreu et al., (DELPHI Collaboration) " A measurement of B mesons production and lifetime using D-lepton events", to be published.

[13] J.J.Hernandez et al., (Particle Data Group), Phys. Lett. B239 (1990) 1.

[14] P.Abreu et al., (DELPHI Collaboration) Zeit. Phys. C53 (1992) 567.

[15] W.Venus, in Proceedings of the Rencontres de Physique de la Vallée d'Aoste, (1992), J.Kroll, in Proceedings of the XXVIIth Rencontres de Moriond (1992).

Figure Captions

- Figure 1: The four diagrams which contribute to $l^{\pm}D_s^{\mp}$ final states and in which the lepton and the D_s are in the same jet. There is no channel for same sign lepton-D_s correlations.
- Figure 2: Monte Carlo simulation of the P_t distribution of the lepton relative to the remaining charged particles in the jet. The shaded areas correspond to events initiated by a B_s^0 decay.
- Figure 3: Mass distributions for $KK\pi$ candidates, accompanied, in the same jet, by a muon of opposite sign with P_t greater than 0.6 GeV/c.
  (a) $\phi\pi$ candidates . (b) $K^{*0}K$ candidates .
  Combined mass distributions for $K^{*0}K$ and $\phi\pi$ candidates:
  (c) $P_t > 0.8$ GeV/c . (d) $P_t > 1.2$ GeV/c .
- Figure 4: $K\pi\pi$ mass distributions used to search for the D^+ mesons remaining after imposing the selections for D_s decays to $K^{*0}K$.
  (a) $K\pi$ mass combination is taken in the K^{*0} region. No request has been applied on the ψ angle distribution, on particle identification and on the flight distance.
  (b) using the same selections as in the D_s analysis
  (c) D_s signal with a 10 MeV/c binning. The shaded area corresponds to events that could come from $D^+ \rightarrow K^-\pi^+\pi^+$.
- Figure 5: $KK\pi$ mass distributions associated to a muon with a P_t larger than 0.8 GeV/c compared to the same distributions obtained in different conditions (shaded)
  (a) selecting same-sign muon-D_s correlations.
  (b) selecting events with $|\cos\psi| \leq 0.5$
  (c) selecting events in the wings of the ϕ and of the K^{*0} signals.
  (d) selecting events in the wings of the ϕ and of the K^{*0} signals and same sign muon-D_s correlations.

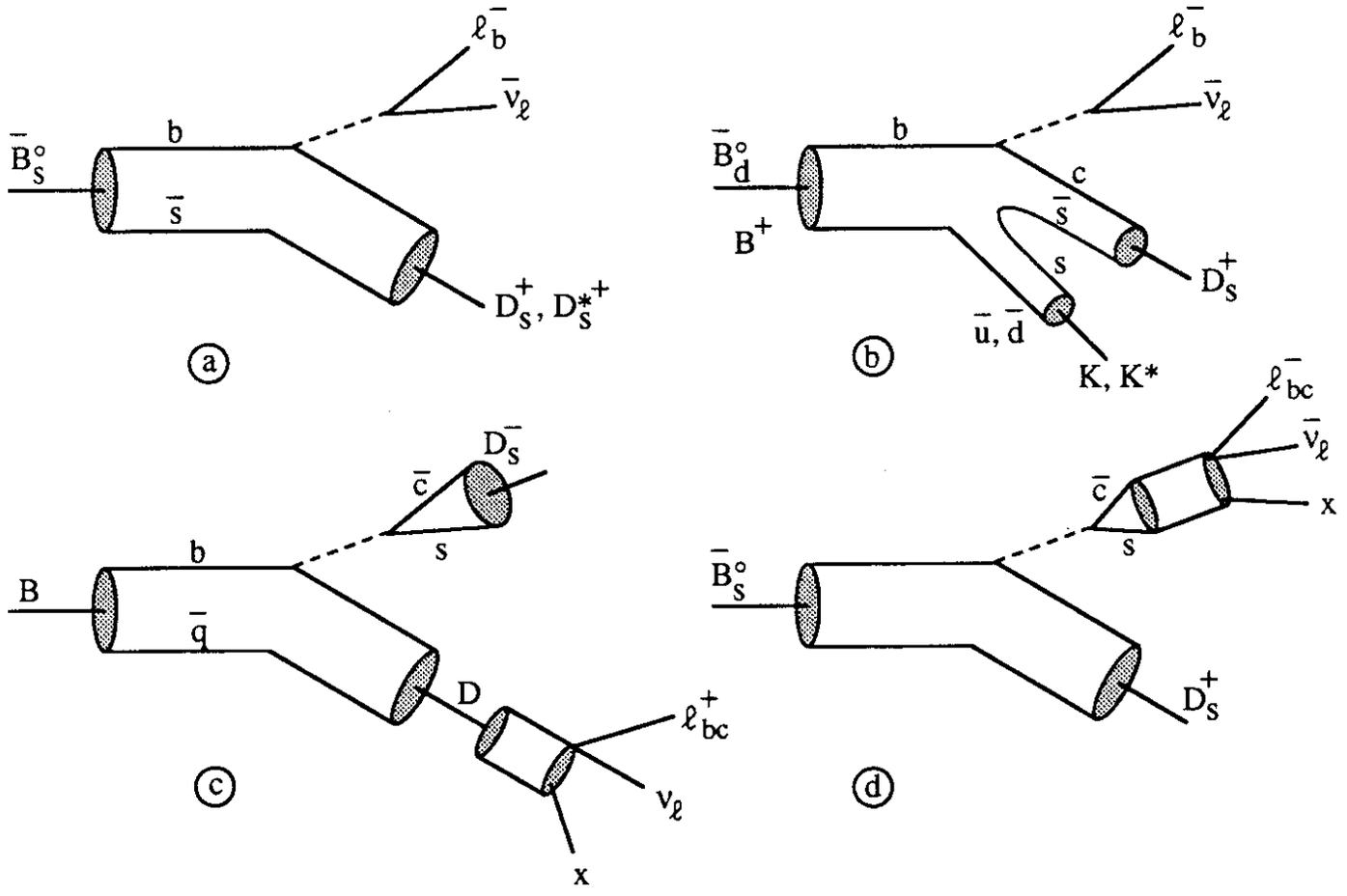
ℓ_b^-
$\bar{\nu}_\ell$
$\bar{B}_s^\circ$
b
$\bar{s}$
D_s^+, D_s^{*+}
a
ℓ_b^-
$\bar{\nu}_\ell$
$\bar{B}_d^\circ$
b
c
B^+
$\bar{s}$
s
D_s^+
$\bar{u}, \bar{d}$
K, K*
b
D_s^-
$\bar{c}$
s
B
b
$\bar{q}$
D
ℓ_{bc}^+
ν_ℓ
x
c
ℓ_{bc}^-
$\bar{\nu}_\ell$
x
s
$\bar{B}_s^\circ$
D_s^+
d

Fig. 1

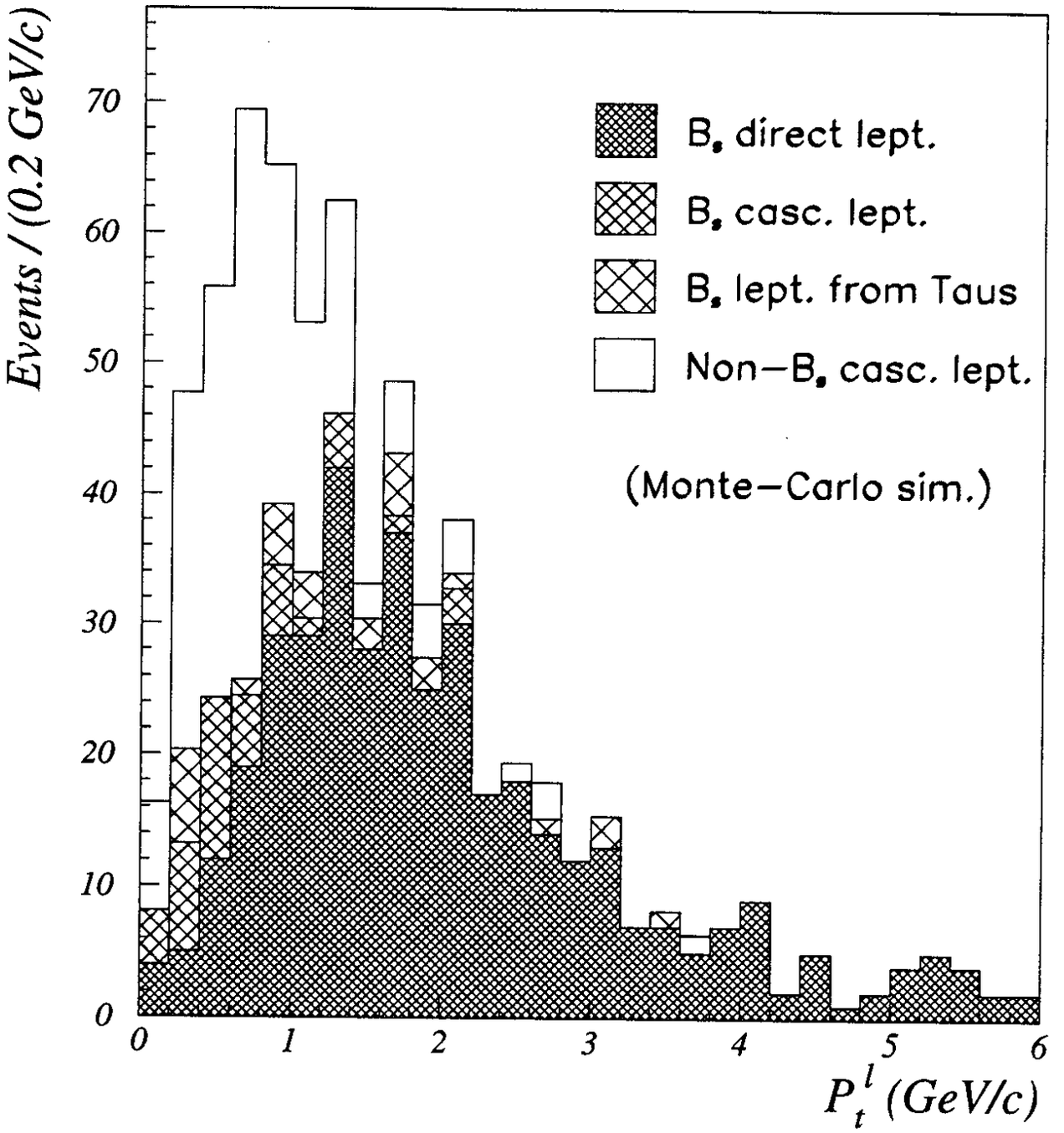
Events / (0.2 GeV/c)
70
60
50
40
30
20
10
0
0
1
2
3
4
5
6
P_t^l (GeV/c)
B, direct lept.
B, casc. lept.
B, lept. from Taus
Non–B, casc. lept.
(Monte–Carlo sim.)

Fig. 2

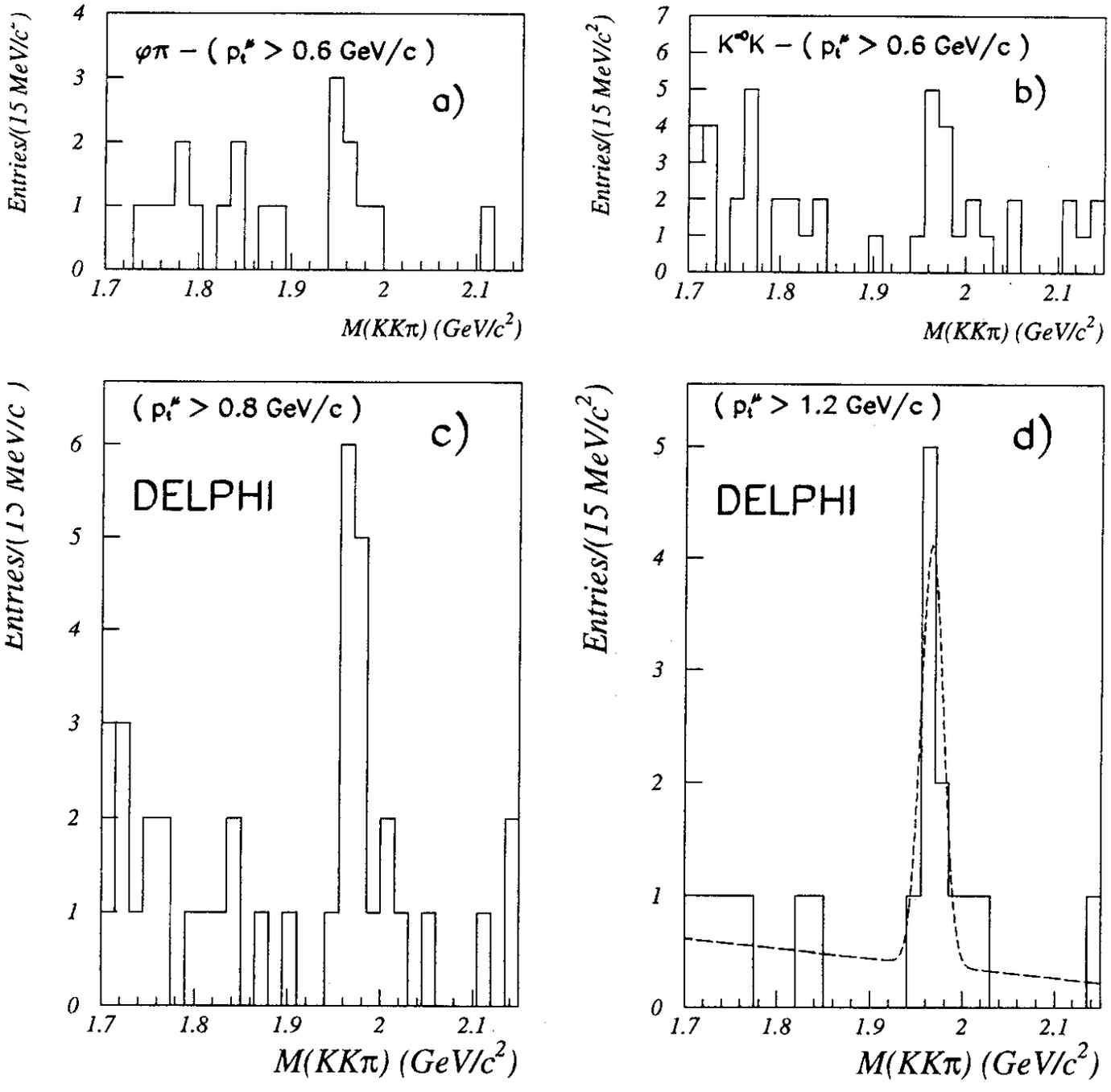
φπ – (p_t^# > 0.6 GeV/c)
a)
K*0K – (p_t^# > 0.6 GeV/c)
b)
(p_t^# > 0.8 GeV/c)
c)
DELPHI
(p_t^# > 1.2 GeV/c)
d)
DELPHI
Entries/(15 MeV/c²)
M(KKπ) (GeV/c²)

Fig. 3

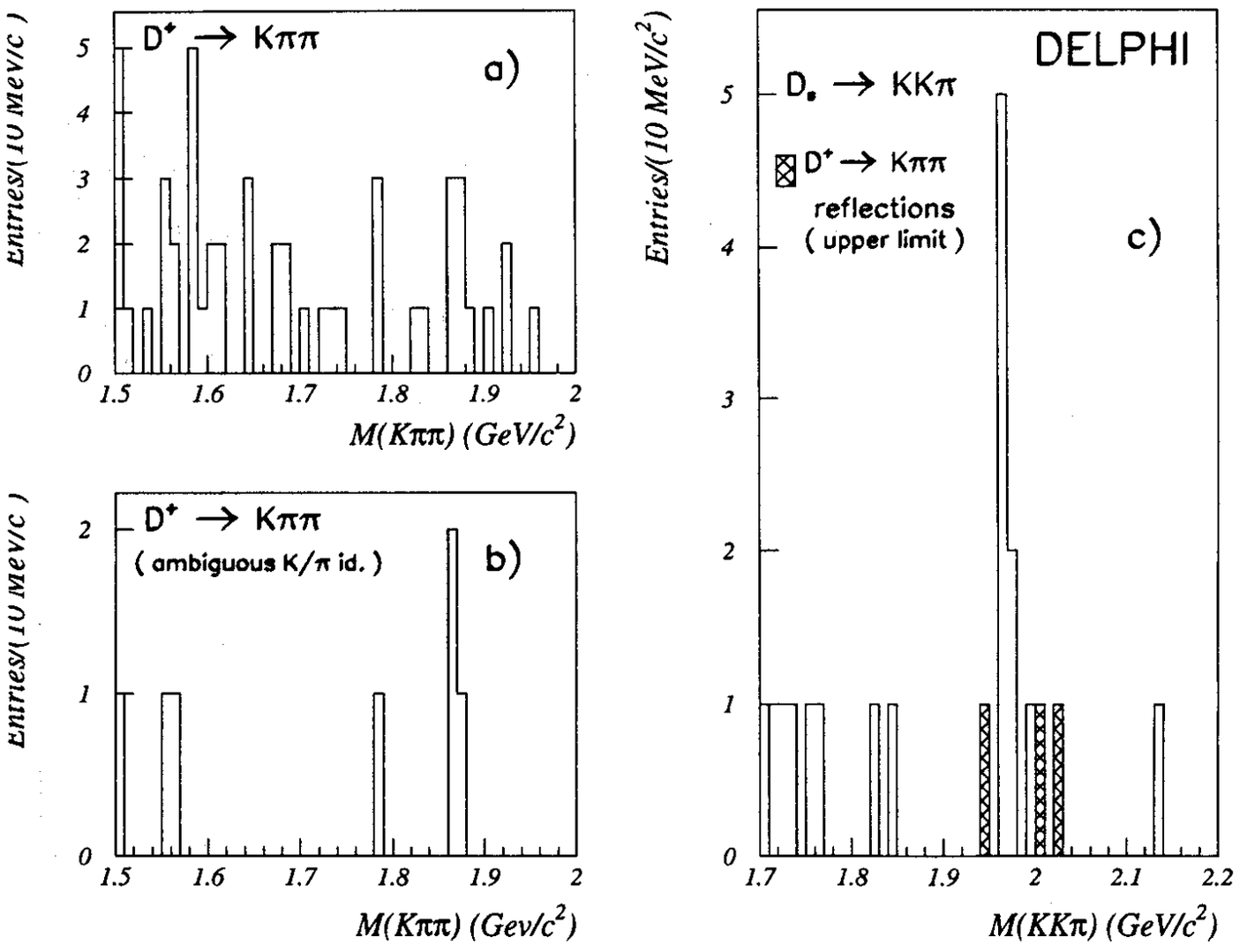
Entries/(10 MeV/c)
D+ → Kππ
a)
M(Kππ) (GeV/c²)
D+ → Kππ
(ambiguous K/π id.)
b)
M(Kππ) (Gev/c²)
Entries/(10 MeV/c²)
DELPHI
Ds → KKπ
D+ → Kππ
reflections
(upper limit)
c)
M(KKπ) (GeV/c²)

Fig. 4

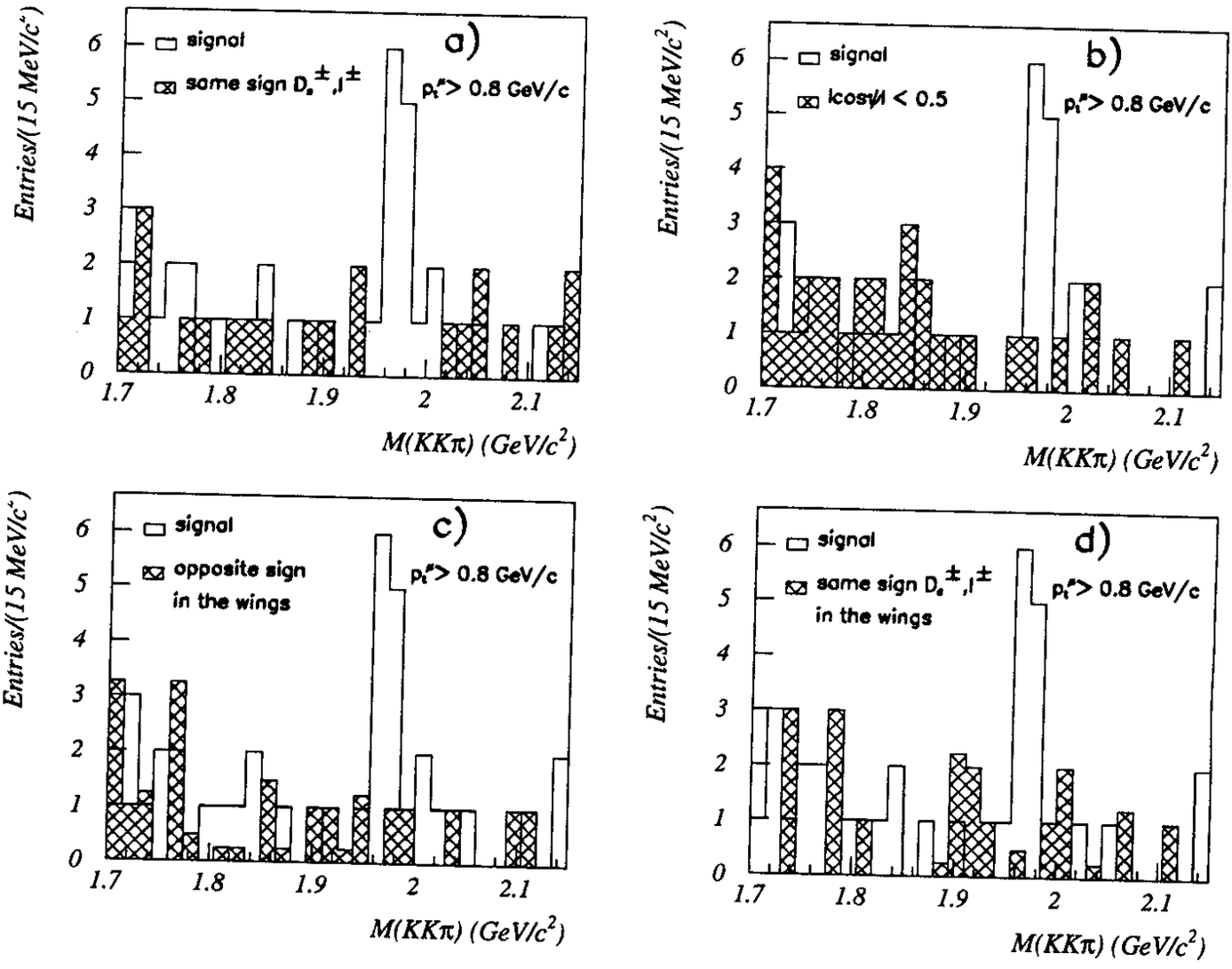
a)
signal
same sign $D_s^{\pm}$,$l^{\pm}$
p_t^{π}> 0.8 GeV/c
b)
signal
|cosψ| < 0.5
p_t^{π}> 0.8 GeV/c
c)
signal
opposite sign
in the wings
p_t^{π}> 0.8 GeV/c
d)
signal
same sign $D_s^{\pm}$,$l^{\pm}$
in the wings
p_t^{π}> 0.8 GeV/c
Entries/(15 MeV/c^2)
M(KKπ) (GeV/c^2)
0
1
2
3
4
5
6
1.7
1.8
1.9
2
2.1

Fig. 5